16th World Conference on Earthquake, 16WCEE 2017

Santiago Chile, January 9th to 13th 2017

Paper N° 2810 (Abstract ID)

Registration Code: S-F1461220828

SHEAR STRENGTH PREDICTION FOR BRITTLE REINFORCED CONCRETE MEMBER CONSIDERING CONCRETE STRESS CONDITIONS

Y. Hibino[(1)], Y. Yamaki[(2)]

[(1)] *Associate Professor, Hiroshima University, hibino@hiroshima-u.ac.jp*
[(2)] *Graduate Student, Hiroshima University, m153953@hiroshima-u.ac.jp*

Abstract

The formula of ultimate shear strength of reinforced concrete members based on truss and arch mechanism is provided in design guideline by Architectural Institute of Japan and which shear design approach are specified in other countries' code. The truss action is comprised of web tension reinforcements combined with a diagonal concrete compression field, and the arch action transfers shear corresponding to concrete stress in compression strut. The shear strength corresponding to web shear reinforcement ratio predicted by the combination of those actions gives feasible ultimate shear strength of beams. However, it is referred that predicted shear strength by the formula tends to overestimate the strength of reinforced concrete columns with low web reinforcement ratio, which show brittle failure. This may indicate that shear transfer mechanism formed in brittle members does not agree with the predicted failure mechanisms in the formula.

In this study, to evaluate failure mechanism of brittle reinforced concrete members, concrete stress condition inside of the members was investigated by carrying out of experimental tests of specimen. The specimen simulates brittle reinforced concrete column which web reinforcement ratio is low. Geometric properties are the same in all specimens; cross section is 180mm×300mm; shear span length is 900mm; and shear span-to-depth ratio is 1.5. Concrete compressive strength and magnitude of axial load were selected as parameter. Cyclic loadings were applied to the specimen with constant axial load correspond to specified magnitudes. Triaxial strain gages were placed in the core of the cross section of columns to measure concrete's strain.

From the experimental test, concrete stress in the concrete core section at ultimate state was evaluated. Predicted Mohr stress circles drawn by measured strain depends on the axial load ratio and concrete strength. Factors associated with Mohr-Coulomb criterion was evaluated with experimental data, and shear strength prediction method was proposed on assumption that the brittle shear failure occurs when Mohr stress circle reaches Mohr-Coulomb criterion, which represents slip failure of concrete. The proposed shear strength agrees with experimental results, however, which gives underestimate strength for the brittle failure specimens with normal strength of concrete.

Keywords: shear strength, concrete stress, brittle failure, Mohr-Coulomb

1. Introduction

A formula predicts ultimate shear strength of reinforced concrete members based on truss and arch actions is provided in design guideline by Architectural Institute of Japan [1] and which shear design approach are specified in other countries' code. The truss action is comprised of web tension reinforcements combined with a diagonal concrete compression field, and the arch action carried by concrete compression strut transfers shear. The shear strength V_u predicted by combination of truss and arch actions gives feasible ultimate shear strength of beams.

$$V_u = 2\rho_{he} f_h b_e j_e + \left(\nu_0 f'_c - \frac{5\rho_{he} f_h}{\lambda}\right)\frac{bh}{2}\tan\theta \tag{1}$$

where ρ_{he} is effective shear reinforcement ratio; f_h is yield strength of shear reinforcement; b_e is effective width; j_e is effective lever arm; f'_c is concrete compressive stress; ν_0 is effective compressive strength factor (=1.72 $f'_c{}^{-0.32}$ MPa); λ is effective truss factor; b is width; h is depth; and θ is angle of concrete compressive strut.

The formula is given for both beams and columns; however, axial load is not considered in this formula. Moreover, it is referred that shear strength predicted by the formula tends to underestimate the shear strength of columns with low web reinforcement ratio and high axial load ratio [1], which column is likely to show brittle failure. This may indicate that the shear transfer mechanism formed inside of members does not agree with the mechanisms assumed by present formula.

On the contrary, shear strength prediction of reinforced concrete members with Mohr-Coulomb criterion was proposed [2, 3]. When Mohr circle stress reaches the criterion internally, shear stress is given [3] (See Fig. 1). The criterion associated with shear stress τ and normal stress σ were defined by the followings.

$$\tau = 0.17 f'_c + 0.75\sigma \tag{2}$$

$$\sigma \le f_t \tag{3}$$

where f_t is tensile stress of concrete.

The ultimate shear strength given by Mohr-Coulomb criterion has theoretical background; however, the proposed theory is not proved with actual concrete stress and the stress condition inside of member subjected to axial and horizontal loads. Furthermore, Pujol [3] addressed that the proposed procedure may be too conservative for column with axial load ratios which is larger than 0.4 and with small amounts of transverse reinforcements. In this study, to investigate shear failure mechanism based on actual stress inside of members, concrete stress condition inside of members was observed with carrying out of experimental tests of reinforced concrete column subjected to non-, low- and high-axial loads, which member demonstrates brittle failure, and the computed strength was compared with experimental results.

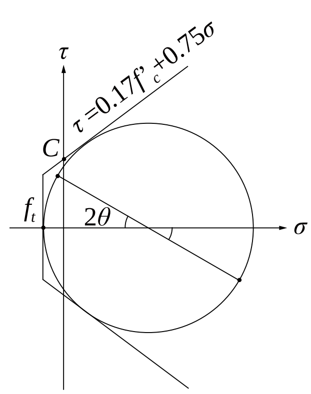

Fig. 1 – Mohr stress circle and Mohr-Coulomb criterion

2. Test specimens

Three series of specimens: AD1; AD2 and AD3, were designed to simulate brittle reinforced concrete column which has small amounts of transverse reinforcements. Geometric properties were the same in all specimens; cross section is 180mm×300mm; shear span length is 900mm; and shear span-to-depth ratio is 1.5. Concrete strength and magnitude of axial load were selected as parameter, which are shown in Table 1. The configuration of the specimen is shown in Fig. 2. The high strength steel bars, D19 were used as longitudinal reinforcement and concrete strength f'_c of 30MPa, 80MPa and 100MPa were used which properties are shown in Table 2 and 3. The transverse reinforcement ratio was arranged so that the column demonstrates brittle shear failure. The concrete stress-strain relationship is shown in Fig. 3. The solid lines in Fig. 3 represent elastic stiffness computed by modulus of elasticity. Bi-directional double-curvature cyclic loadings were applied to the specimen under constant axial load P which simulates gravity load with specified magnitude: P/bhf'_c=0; 0.2; and 0.4. The loading program was controlled by drift angle R which is given by the relative lateral displacement of column divided by its height L. The target drift ratio was ±0.125%×2, ±0.25%×2, ±0.5%×2, ±1%×2, ±1.5%×2, and ±2%×2. To measure the strain of concrete, acrylic bars triaxial strain gages were glued on it were placed in the core section of columns as shown in Fig. 4. The acrylic bars have serrate configuration to improve bond performance with concrete. The numbers on Fig. 4 indicate ID of the strain gage's position.

Table 1 – Specimens properties

<table>
<tr><th>Series</th><th>Specimen</th><th>b (mm)</th><th>h (mm)</th><th>L (mm)</th><th>M/Vh</th><th>Longitudinal reinforcement</th><th>Shear reinforcement</th><th>P/bhf´_c</th><th>V_u (kN)</th></tr>
<tr><td rowspan="3">AD1</td><td>AD1-0</td><td rowspan="9">180</td><td rowspan="9">300</td><td rowspan="9">900</td><td rowspan="9">1.5</td><td rowspan="9">4-D19 (ρ_t=1.18%)</td><td rowspan="3">D6@220 (ρ_h=0.16%)</td><td>0</td><td rowspan="3">93.7</td></tr>
<tr><td>AD1-2</td><td>0.2</td></tr>
<tr><td>AD1-4</td><td>0.4</td></tr>
<tr><td rowspan="3">AD2</td><td>AD2-0</td><td rowspan="3">D6@360 (ρ_h=0.10%)</td><td>0</td><td rowspan="3">147.1</td></tr>
<tr><td>AD2-2</td><td>0.2</td></tr>
<tr><td>AD2-4</td><td>0.4</td></tr>
<tr><td rowspan="3">AD3</td><td>AD3-0</td><td rowspan="3">D6@380 (ρ_h=0.09%)</td><td>0</td><td rowspan="3">166.6</td></tr>
<tr><td>AD3-2</td><td>0.2</td></tr>
<tr><td>AD3-4</td><td>0.4</td></tr>
</table>

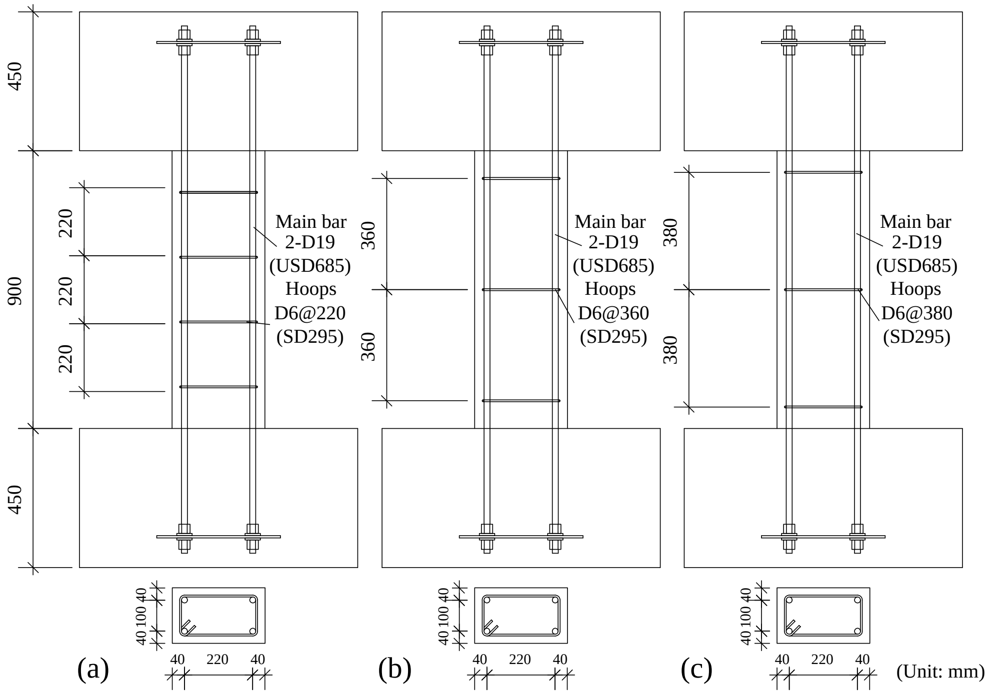

Fig. 2 – Configuration of specimens

Table 2 – Steel properties

No.	Strength	Yield strength (MPa)	Yield strain (μ)	Tensile strength f_t (MPa)	Modulus of elasticity (GPa)
D19	USD685	720	3952	901	182
D6	SD295A	404	4028	558	204

Table 3 – Concrete properties

Series	Compressive strength, f'_c (MPa)	Tensile strength, f_t (MPa)	Modulus of elasticity (GPa)
AD1	30.8	2.84	24.5
AD2	80.8	5.41	41.6
AD3	100.0	5.90	41.3

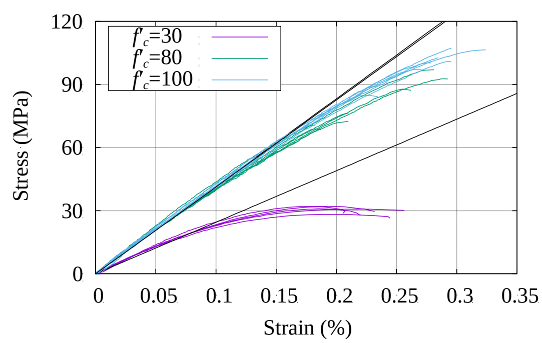

Fig. 3 – Stress-strain relationship of concrete

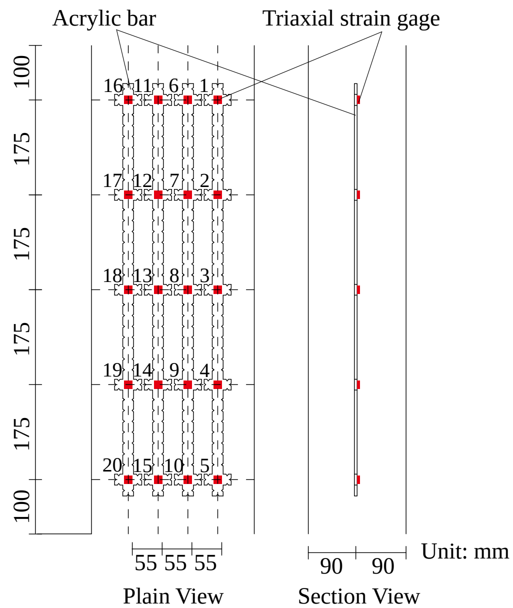

Fig. 4 – Configuration of acrylic bars

3. Experimental results

2.1 Load-deflection response, cracks and strength

The load deflection response of the specimens is shown in Fig. 5. The maximum lateral load increases with increasing of axial load ratio and concrete strength except the maximum load of the specimen AD3-2 which is lower than that of the specimen AD2-2. The lateral load after the maximum point drastically decreased due to the shear failure for all the specimens and all the specimens demonstrated brittle failure. The maximum lateral load $V_{\max}$ and drift angle at the failure, $R_{\max}$ are shown in Table 4.

The observed crack patterns are depicted in Fig. 6. Diagonal wide cracks were observed and similar cracks occurred in all the specimens; however, almost the wide diagonal crack's shapes were dogleg. The cause of this diagonal cracks may be due to fine cracks caused by autogenous shrinkage after casting and small misalignment between applied axial load point and the center of the cross section.

Table 4 shows both observed and classified failure types [4]: shear tension (ST) failure; shear compression (SC) failure; diagonal tension (DT) failure. The ST failure is defined as the shear failure with yielding of shear reinforcement, the SC failure is defined as the shear failure with compression failure of concrete without yielding of shear reinforcement, and the DT failure is defined as the shear failure with diagonal shear crack and drastic degradation of lateral load. The failure types were classified by following procedure: if shear crack strength V_{cr} is larger than V_u, failure type is classified into DT failure; and in the reverse case, failure types are classified into ST or SC failure. This procedure is based on an assumption that if shear crack strength V_{cr} is larger than ultimate shear strength V_u, the shear crack strength governs the maximum strength. The shear crack strength V_{cr} [1] derived from theoretical model are given by following, which are shown in Table 4.

$$V_{cr} = \frac{bh}{1.5}\sqrt{f_t^2 + \frac{f_t P}{bhf_c'}} \tag{4}$$

For the specimen AD1-0 and AD2-0, both observed failure types were ST failure because drastic decrease in load carrying capacity with yielding of shear reinforcement was observed. On the other hand, for the specimen AD2-2, failure type was SC failure because yielding of shear reinforcement was not observed. For the other specimens, diagonal shear crack appeared with drastic shear deterioration, therefore observed failure type was DT failure. Then, observed failure types of the specimen with low axial load ratio were ST or SC failures, although classified failure types for all the specimen were DT failure because shear crack strength V_{cr} shown in Table 4 are larger than computed shear strength V_u shown in Table 1. Fig. 7 shows comparison of experimental results $V_{\max}$, V_{cr} and V_u. The shear crack strength V_{cr} overestimates measured shear strength for all the specimens except AD1-0, and the shear strength V_u underestimates the shear strength except the specimen AD3-0. This disagreement between computed and measured shear strength represents that DT failure can be determined by neither tension failure of concrete assumed in the shear crack strength V_{cr} nor compression failure of concrete assumed in the ultimate shear strength V_u.

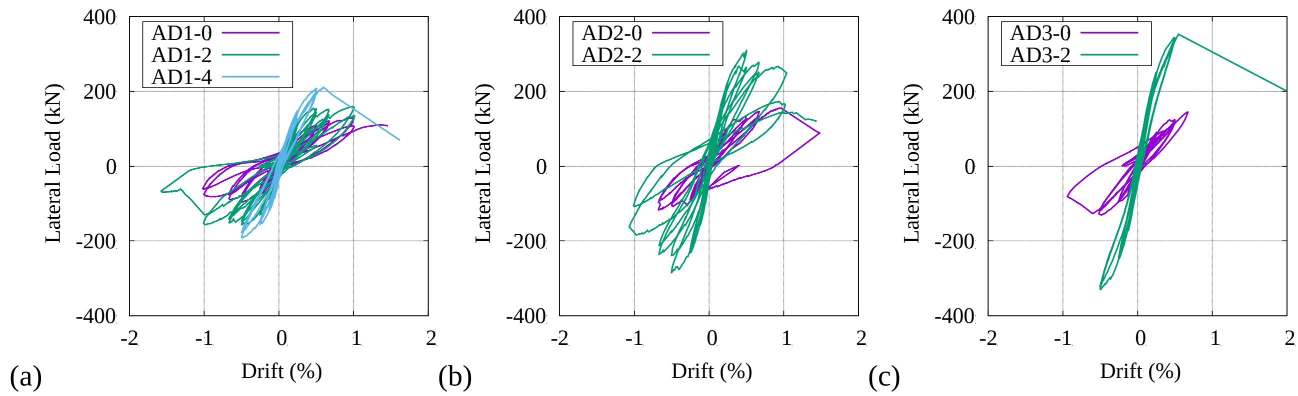

Fig. 5 – Lateral load-drift relationship: (a) AD1 series, (b) AD2 series, (c) AD3 series

Fig. 6 – Crack patterns: (a) AD1-0, (b) AD1-2, (c) AD1-4, (d) AD2-0, (e) AD2-2, (f) AD3-0, (g) AD3-2

Table 4 – Strength and failure type of specimen

Series	Specimen	$V_{\max}$ (kN)	$R_{\max}$ (%)	Failure Type		V_{cr} (kN)	Gage No.
				Observation	Classification [4]		
AD1	AD1-0	128.7	0.97	ST		102.2	8, 13, 14
	AD1-2	159.8	0.99	DT		182.0	8, 13, 14, 19
	AD1-4	211.1	0.60	DT		236.2	7, 8, 14, 19
AD2	AD2-0	155.9	0.96	ST	DT	236.2	14, 19
	AD2-2	307.7	0.50	SC		388.9	7, 8, 13, 14, 19
AD3	AD3-0	145.1	0.96	DT		212.4	7, 8, 13, 14, 19
	AD3-2	352.8	0.55	DT		445.1	2, 8, 13, 14, 19

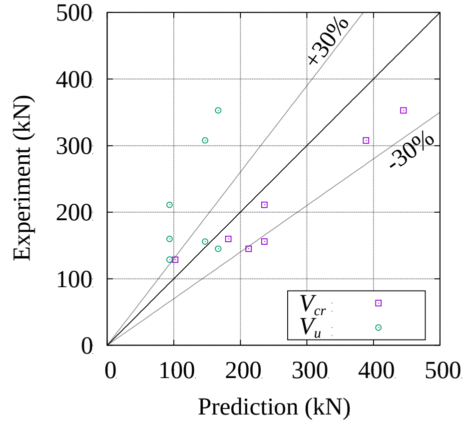

Fig. 7 – Comparison of maximum shear strength $V_{\max}$, V_{cr} and V_u

2.2 Principal stresses of core concrete

The maximum principal stress $\sigma_{\max}$ and minimum stress $\sigma_{\min}$ of core concrete measured by triaxial strain gages were derived by following equations.

$$\sigma_{\max} = \frac{E_c}{1-\nu^2}(\epsilon_{\max} + \nu\epsilon_{\min}) \tag{5}$$

$$\sigma_{\min} = \frac{E_c}{1-\nu^2}(\epsilon_{\min} + \nu\epsilon_{\max}) \tag{6}$$

where $\varepsilon_{\max}$ is maximum principal strain; $\varepsilon_{\min}$ is minimum principal strain; ν is Poisson's ratio (=0.2). The principal strains were calculated by measured strains using rosette analysis. Note that stress-strain characteristic of concrete was idealized by elastic perfectly plastic approximation. Although small gap was observed between the stress estimated with modulus of elasticity and measured stress of concrete in the range of higher strain larger than 0.125 for the concrete of f'_c =30 MPa as shown in Fig. 3, the elastic stiffness of high strength concrete was almost idealized by modulus of elasticity.

Fig. 8 shows the Mohr stress circle and Mohr-Coulomb criterion with maximum and minimum principal stresses obtained by measured strains at the maximum load, which numbers correspond to ID of strain gages shown in Fig. 4 and used gage numbers are shown in Table 2. The solid straight lines represent the failure criteria defined by Eq. 2 and 3 and if the circle reaches the criterion, concrete fails in shear slip and tension failure are assumed. Note that the circles which both principal stresses showed compressive value were excluded from consideration because it was unrealistic condition which was assumed to be due to error of measured strain. Most of the circle's stress exceeds the criterion of concrete tensile strength (Eq. 2) and some of the circle has small diameter. Especially, small circles are observed on the specimen with non- and low- axial load ratio (e.g. P/bhf'_c = 0 and 0.2). For the specimen AD1 series, the maximum and minimum principal stress increased with increasing of axial load ratio. On the other hand, for the specimen AD2-0, little stress circle was drawn due to error of strain gages. The circles of No.7 on the specimen AD2-2 and No.2 on the specimen AD3-2 reach the Mohr-Coulomb criterion (Eq. 2). For the specimen AD3 series, large stress circles were drawn on the specimen AD3-2 which axial load ratio is larger than that of the specimen AD3-1. Because the center of the circle was decreased according to increasing of axial load ratio, the larger the axial load ratio becomes, the larger minimum principal stress becomes. By considering expansion of Mohr stress circle and Mohr-Coulomb criterion, ultimate shear strength of reinforced concrete column shows brittle failure can be predicted.

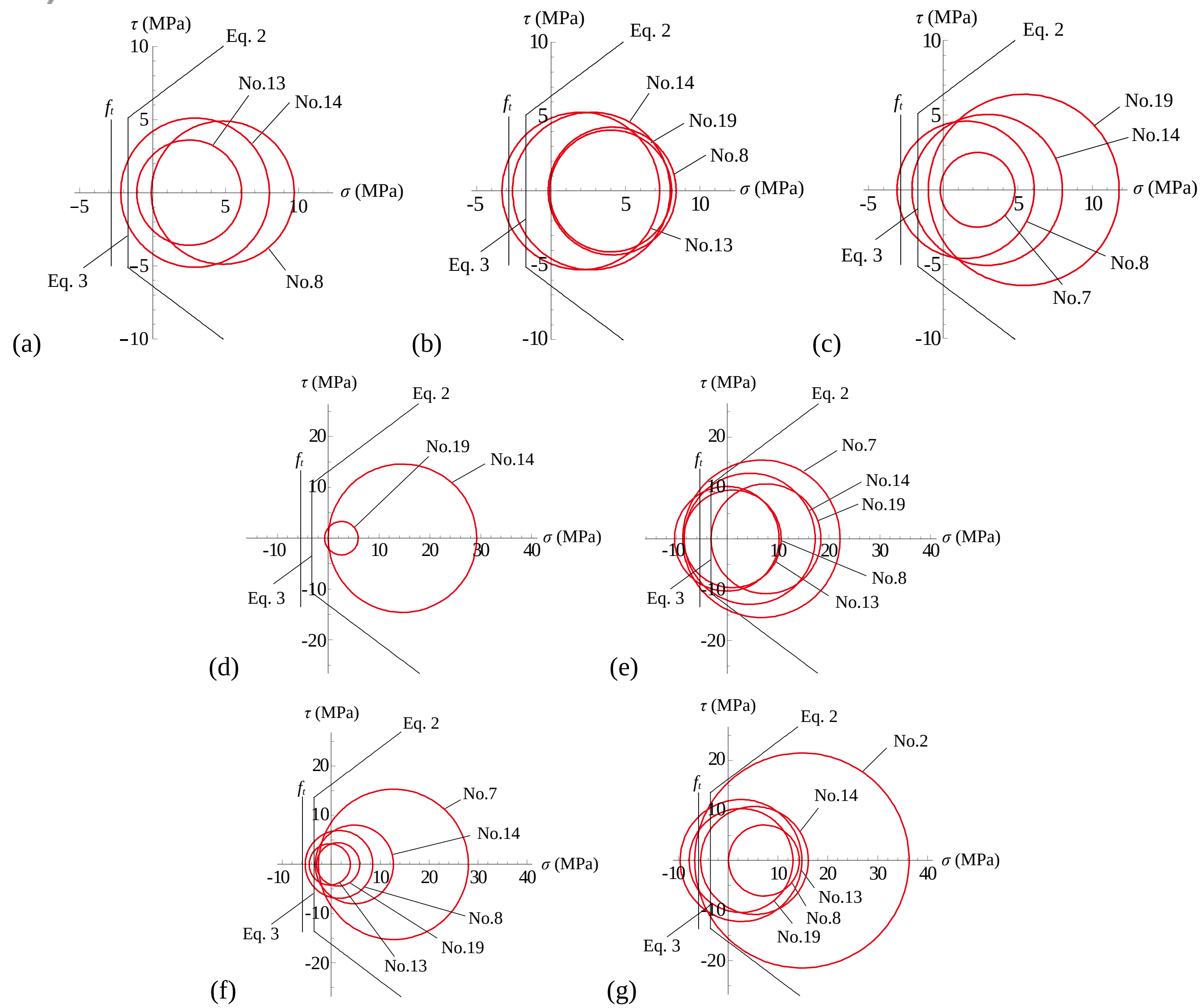

Fig. 8 – Mohr stress circle: (a) AD1-0, (b) AD1-2, (c) AD1-4, (d) AD2-0, (e) AD2-2, (f) AD3-0, (g) AD3-2

2.3 Factors of Mohr-Coulomb criterion

Some of the Mohr circle stress exceeds the criteria given by Eqs. 2 and 3, and for the specimen with non- and low-axial load ratios, the stress circle did not reach both criteria. Then, if it can be assumed that drawn stress circle satisfy the failure criterion when brittle failure occurs, the circle should reach both criteria. Therefore, the modified criteria at the brittle failure can be predicted.

The cohesion *C* (See Fig. 1) was obtained from the intercept of tangent line of the stress circle with the same slope of Eq. 2, that is, the criterion moves in parallel. Fig. 9 shows the relationship between normalized cohesion C/f'_c and crack width *w*. The horizontal solid line in the graph indicates cohesion C/f'_c =0.17 defined in Eq. 2. Normalized cohesion tends to decrease with increasing of crack width, which indicates that cohesion of cracked concrete decreases. Similarly, the decreasing of cohesion was evaluated with drift of shear failure and shear span length [3]. Upper boundary line of C/f'_c in terms of crack width was approximated by Eq. 7, which C/f'_c is less than 0.25 and crack width is less than 3 mm considering upper limit of cohesion is 0.25 [3].

$$\frac{C}{f'_c} = \min(0.17, 0.25 - 0.83w) \geq 0 \tag{7}$$

where the stresses are in MPa and w is crack width in mm.

Maximum crack width w of reinforced concrete column can be predicted by drift angle R [5].

$$w = 1.5R \tag{8}$$

where the crack width in mm and drift angle is in %.

Hence, decreasing of cohesion can be predicted by Eqs. 7 and 8. Fig. 10 shows relationship between normalized minimum principal stress σ_{min}/f_t, and principal tensile strain. The minimum principal stress is obtained by triaxial strain gages shown in Table 4. Some of normalized minimum principal stress are greater than concrete tensile strength f_t and large dispersion is observed. The solid curve which is given by following equation [6].

$$\sigma_{\min}/f_t = \frac{1}{1+\sqrt{200\epsilon}} \tag{9}$$

In this study normalized principal stress of 0.83 was assumed by Eq. 9 with average strain of 0.2×10^{-3} obtained by data in the range of σ_{min}/f_t <1.0.

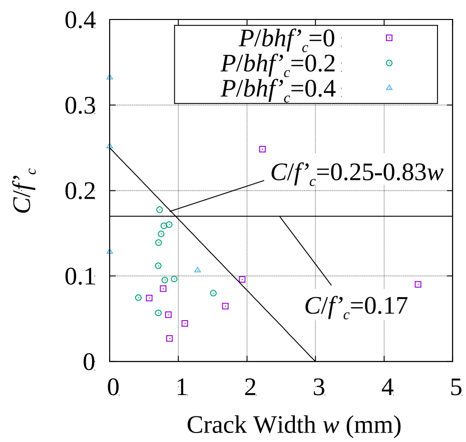

Fig. 9 – Relationship between C/f'_c and crack width w

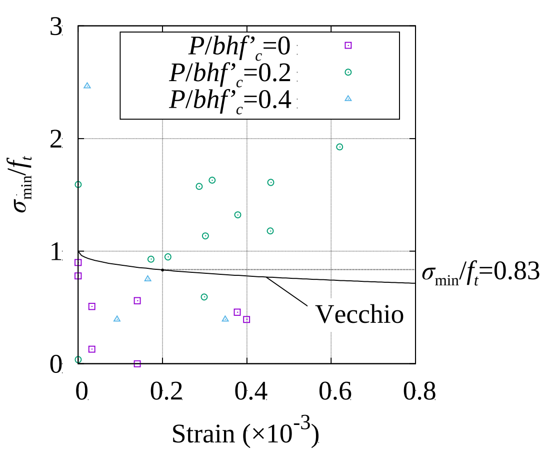

Fig. 10 – Relationship between σ_{min}/f_t and strain

3. Prediction of ultimate shear strength

Ultimate shear strength V_m with Mohr stress circle was assumed by following.

$$V_m = \tau_{\max} \sin 2\theta \cdot b_c h_c \tag{10}$$

where $\tau_{\max}$ is maximum shear stress obtained by Mohr stress circle; b_c is core concrete width; h_c is core concrete depth; and θ is angle of concrete compression strut [7] given by

$$\theta = \operatorname{atan}\frac{h-c}{L} = \operatorname{atan}\frac{\left(0.75+\frac{2P}{bhf'_c}\right)h}{L} \tag{11}$$

where c is neutral axis depth.

The ultimate shear strength V_m is derived assuming that concrete compression strut formed in member and the stress circle reaches Mohr-Coulomb criterion when failure occurs. It is assumed that the cover concrete does not effective for shear resistance as addressed by Pujol [3]. The effect of axial load on shear strength is considered by shift of neutral axis depth $c=h(0.25+0.5P/bhf'_c)$ [7]. Fig. 11 shows comparison of computed shear strength V_m with maximum shear stress on Mohr stress circle and experimental result. The computed strength underestimates the experimental results. Then, shear stress at the ultimate state was predicted by Mohr stress circle assuming that the circle reaches both modified criteria determined by Eqs. 7 to 11. Fig. 12 shows relationship between experimental result and computed shear strength with modified stress circle. Computed strength agrees with experimental results for the specimens AD2-2 and AD3-2; however, for the specimen AD1 series, computed strength underestimates experimental result. For more accurate estimation, the expression of ultimate shear strength based on shear stress should be reconsidered and confirmed.

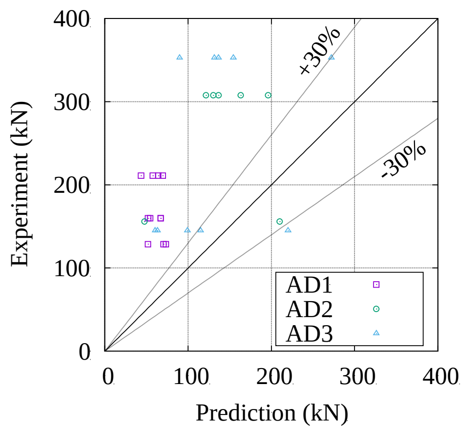

Fig. 11 – Comparison of shear strength and experiment

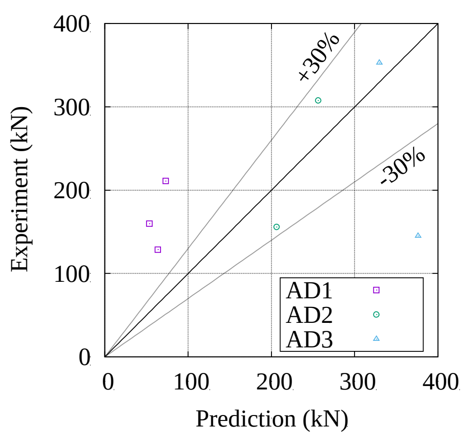

Fig. 12 – Comparison of computed shear strength and experiment

4. Conclusions

In this study, concrete stress conditions inside of reinforced concrete column showed brittle shear failure was investigated. The concrete stress inside of members was assumed by strain measured during experimental tests. The following conclusions are summarized: 1) Mohr stress circle drawn by concrete stress showed different diameter and shape according to the axial load ratio; 2) Diameter of Mohr stress circle of specimen with high axial load ratio became lager than that of the specimen with lower axial load ratio; 3) Modified Mohr-Coulomb criteria which can represent a criteria at brittle failure which is assumed as of shear slip failure of concrete; 4) Proposed ultimate shear strength given by Mohr stress circle with modified Mohr-Coulomb criterions agreed with experimental results; however, for the specimen with normal strength concrete, the predicted strength gave underestimation. It is shown that proposed procedure may give ultimate shear strength of brittle reinforced concrete members.

5. References

[1] Architectural Institute of Japan (1999): *Design Guidelines for Earthquake Resistant Reinforced Concrete Buildings Based on Inelastic Displacement Concept*, Architectural Institute of Japan. (in Japanese)

[2] Pujol S, Sozen M, Ramirez J (2000): Transverse Reinforcement for Columns of RC Frames to Resist Earthquakes. *Journal of Structural Engineering*, ASCE, **126** (4), 461-466.

[3] Pujol S, Hanai N, Ichinose T, Sozen M A. (2016): Using Mohr-Coulomb Criterion to Estimate Shear Strength of Reinforced Concrete Columns, *ACI Structural Journal*, American Concrete Institute, **113** (3) 459-468.

[4] Uchiyama M, Sakashita M, Kono S, Nishiyama (2012): Shear Capacity of Post-Tensioned Precast Concrete Columns (Part 2 Test Results and Discussions), *Summaries of technical papers of annual meeting 2012*, Architectural Institute of Japan, 935-936. (in Japanese)

[5] Takahashi N, and Nakano Y (2009): A Study on Seismic Repair Cost of R/C Building Structures Using A Geometrical Damage Estimation Model of R/C Members, *Proceedings of the Eighth International Symposium on New Technologies for Urban Safety of Mega Cities in Asia*, Incheon, Korea, 313-322.

[6] Vecchio F J, and Collins M. P (1986): The Modified Compression-Field Theory for Reinforced Concrete Elements Subjected to Shear, *ACI Journal Proceedings*, **83** (2) 219-231.

[7] Hibino Y, Hisada M, Shinohara Y, Hayashi S (2012): Shear Strength of Reinforced Concrete Columns with Low Web Reinforcement Considering Compressive Strut Shape, *Journal Structural and Construction Engineering*, Architectural Institute of Japan, **77** (677) 1113-1122. (in Japanese)